Tree Instance Segmentation and Traits Estimation for Forestry Environments Exploiting LiDAR Data Collected by Mobile Robots

Meher V. R. Malladi Tiziano Guadagnino Luca Lobefaro Matias Mattamala Holger Griess
Janine Schweier Nived Chebrolu Maurice Fallon Jens Behley Cyrill Stachniss

***Abstract*— Forests play a crucial role in our ecosystems, functioning as carbon sinks, climate stabilizers, biodiversity hubs, and sources of wood. By the very nature of their scale, monitoring and maintaining forests is a challenging task. Robotics in forestry can have the potential for substantial automation toward efficient and sustainable foresting practices. In this paper, we address the problem of automatically producing a forest inventory by exploiting LiDAR data collected by a mobile platform. To construct an inventory, we first extract tree instances from point clouds. Then, we process each instance to extract forestry inventory information. Our approach provides the per-tree geometric trait of "diameter at breast height" together with the individual tree locations in a plot. We validate our results against manual measurements collected by foresters during field trials. Our experiments show strong segmentation and tree trait estimation performance, underlining the potential for automating forestry services. Results furthermore show a superior performance compared to the popular baseline methods used in this domain.**

I. Introduction

Forests are vital for our ecosystems [10]. They support critical processes like carbon sequestration and biodiversity in the biosphere, while also providing resources for timber industries and offering opportunities for human leisure in the anthroposphere [10], [27]. Monitoring and documenting the status of a forest are time-intensive tasks while the number of forests is decreasing in most countries. Robots, however, can perform extensive data collection in forests and may go in the future as far as realizing automated maintenance and even tree harvesting. Monitoring can yield precise information on tree count, species distribution, essential geometric traits like diameter at breast height (DBH), and more, constituting a forest inventory [20]. Foresters can use such detailed inventories to make accurate forecasts of stand growth, plan harvesting strategies, optimize species rotation cycles, and more, contributing to effective and sustainable foresting practices [29].

Meher V. R. Malladi, Tiziano Guadagnino, Luca Lobefaro, Jens Behley, and Cyrill Stachniss are with the Center for Robotics, University of Bonn, Germany. Cyrill Stachniss is additionally with the Department of Engineering Science at the University of Oxford, UK, and with the Lamarr Institute for Machine Learning and Artificial Intelligence, Germany. Matias Mattamala, Nived Chebrolu and Maurice Fallon are with the University of Oxford, UK. Holger Griess and Janine Schweier are with Swiss Federal Institute for Forest, Snow and Landscape Research, Switzerland.

This work has partially been funded by the European Union's Horizon Europe research and innovation program under grant agreement No 101070405 (DigiForest), by the Deutsche Forschungsgemeinschaft (DFG, German Research Foundation) under Germany's Excellence Strategy, EXC-2070 – 390732324 – PhenoRob and by the Swiss State Secretariat for Education, Research and Innovation (SERI).

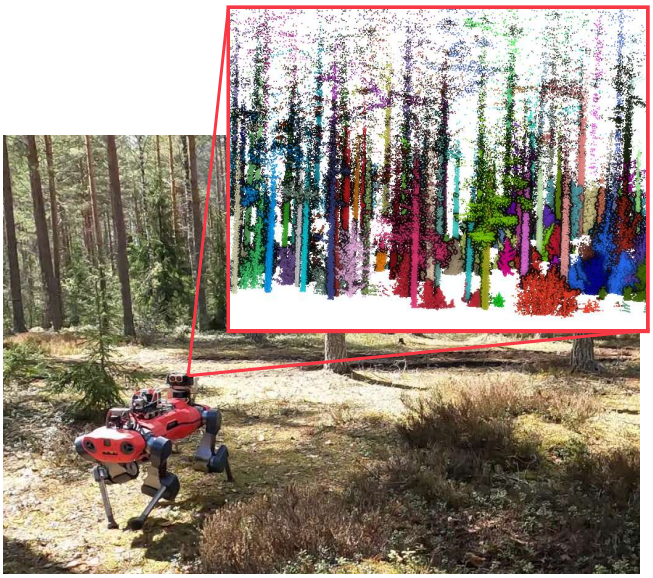

Fig. 1: Instance segmentation results on data collected with a mobile robotics platform in a forest near Evo, Finland. On the left, we show the ANYmal platform, which was used for data collection, and on the right the segmentation results of our approach on the collected data. Different colors of points indicate different instances.

Common sensor modalities for forest inventory include terrestrial laser scanners (TLS) [19] and UAV laser scanners [43]. TLS offers high resolution at the cost of limited spatial coverage, while UAV laser scanners have lower resolution but with larger coverage. Additionally, since UAV flights are usually performed above-canopy, occlusions can result in insufficient tree trunk detail. By using ground-based robotic platforms and below-canopy UAV flights, both problems of spatial coverage and trunk-canopy detail can be addressed. Although their resolution might not match TLS, they can still provide sufficient below-canopy detail and extended spatial extent.

This paper focuses on the problem of using laser scanner data collected with mobile robotic platforms to automate forest inventory: to obtain forest stand tree count and per-tree information like DBH. DBH, measured approximately 1.3 m above ground, is considered the most crucial parameter in forestry [20]. It is used in estimating forest biomass [23], developing forest growth models and more [21]. Hence, we developed our approach focusing first on DBH estimation. Within this context, the challenge involves two key aspects. Firstly, the instance segmentation of trees and secondly,

the subsequent modeling of these identified tree instances. Existing methods to address them predominantly work with modalities like airborne laser scanners [5] or TLS [6], [8], [42] and usually take a geometric approach. While modern deep-learning methods have seen good success in related fields [25], [33] and have recently been explored in forestry settings as well [9], [17], [26], they can suffer from problems of out-of-distribution error, differences in sensor platforms between training and testing, differences in forest structure and species distribution, and more. The difficulty is further compounded by the limited availability of open datasets, with the one from Hannah et al. [43] being one of few easily available datasets providing labeled terrestrial, aerial, and UAV laser scanner data. To the best of our knowledge, no labeled datasets from mobile laser scanning platforms are currently available.

The main contribution of this paper is a geometric tree instance segmentation and structural analysis pipeline for forestry data collected from mobile laser scanning platforms. Fig. 1 depicts an example of the type of data considered. Our geometric approach avoids the need for extensive data labeling, as would be needed for modern deep-learning models. With a limited number of parameters, our approach is simple to tune. The proposed method performs well when evaluated quantitatively for segmentation accuracy, DBH trait estimation, and shows good qualitative performance on data collected from varied sensor types. In sum, we make three key claims: Our approach is able to (i) segment trees from mobile laser scans of forest scenes with high segmentation accuracy and no or minimal labeling effort, (ii) fit geometric primitives to the data reliant on the results of the segmentation and achieve high accuracy on tree trait estimation, (iii) show a solid generalization performance across data from different sensor types. These claims are backed up by the paper and our experimental evaluation. The open-source implementation of our approach is available at: `https://github.com/PRBonn/forest_inventory_pipeline`.

II. Related Work

Building maps of the environment from sensor data requires addressing the SLAM problem [11], [37] involving several subtasks such as incremental pose estimation [40], place recognition [41], loop closing [12], and optmization [2], [32]. Using laser scanning to map and study forests has been extensively studied [30], [44], with considerable attention given to airborne laser scanner [5], [18], [34], [38] and TLS data [1], [6], [8], [19], [20], [26], [42], [43]. Mobile laser scanning has only recently become a more viable approach, usually in the form of handheld or UAV platforms [3], [7], [22], [30]. For example, Proudman et al. [30] showcase a SLAM pipeline to enable real-time mapping of forests while simultaneously giving foresters insight into the captured tree structure. We aim to do similarly, to segment trees automatically and analyze traits while working with data collected from mobile robotic platforms, a first in literature to the best of our knowledge.

A standard approach for segmentation of airborne laser scanning data is that of Dalponte et al. [5] in which they rasterize a canopy height model derived from a point cloud, identify local maxima as treetops, and then use a region-growing algorithm to delineate trees. Silva et al. [36] take a similar approach while working with rasterized canopy height models. However, the rasterization can introduce approximation errors that degrades segmentation performance. In contrast, Li et al. [18] work directly on the point cloud, starting from the highest points and using a spacing threshold to iteratively assign points within a search radius to an instance. Both methods have been implemented as part of lidR [34], a popular package for airborne laser data analyses. Similarly, various approaches have been developed for TLS as well, but they critically rely on the high resolution of TLS [6], [8] or require manual interventions [1].

Proudman et al. [30] uses standard Euclidean clustering of locally aggregated mobile laser scans for an initial segmentation and a heuristics-based merge/discard scheme to find tree instances. They estimate DBH via a RANSAC-based circle fit. However, a more sophisticated segmentation approach is necessary when working with complex forest scenes, especially when thickly intertwining canopies exist. Circle fitting for DBH estimation is also done by Heo et al. [13], though they manually segment trees before their analysis. Most related to our approach is the one by Donager et al. [7], who also compare data collected from handheld platforms against TLS and airborne lasers for forest inventory. They show the potential of handheld sensors, reasoning that such platforms overcome the problem of occlusion apparent in TLS. From a slice of the point cloud around breast height, they first identify tree stems by thresholding rasters of geometric features and then clipping out regions. The DBH is estimated by RANSAC cylinder fitting through these points. The tree instances are then "grown" by converting the point cloud into a proximity graph and assigning points to identified stems based on the shortest path in this graph. We take a different approach to segmentation, exploiting the spatial density of points and similarly estimating DBH by cylinder fitting. In contrast to their work, we use a wider height range of points and refine cylinder fitting using a least-squares scheme.

Data-driven techniques have been applied to tackle forestry problems [9], [26], [35], [38], however, the limited availability of labeled point cloud datasets is to the detriment of such approaches. Only a few are openly available for TLS [19], [43], and to the best of our knowledge, none are available with data from mobile platforms. Krisanski et al. [17] used a PointNet++ [31] model for semantic segmentation trained on a mix of data from different sensor types. In a follow-up work [16], they extend their approach to calculate tree count and DBH estimates to be used for forest inventory. Once an input point cloud has been semantically segmented, they filter for stem-only points, cluster short vertical slices using HDBSCAN [24], and by treating these slices as cylinders estimate the radius using a RANSAC circle fit. Stem instances are obtained by merging cylinders

using geometric heuristics. They estimate the DBH by taking a mean of the cylinder radii between 1.0 m and 1.6 m above ground.

We propose in this paper a pipeline for geometric instance segmentation and DBH estimation of trees from robotic mobile laser scans, avoiding the need for extensive data labeling as it would be needed for a data-driven learning approach. We show improved performance on multiple baselines in our segmentation accuracy and DBH estimation evaluations. In conjunction with using mobile laser scans to cover large swathes of forest regions, our proposed pipeline to build forest inventories is a more affordable solution than manual alternatives with human operators and TLS.

III. Our Approach to Forest Inventory

Our pipeline is designed to work on raw aggregated point clouds from LiDAR sensors and automate tree-level analysis to produce an accurate forest inventory. We first focus on the problems of tree instance segmentation and subsequently DBH measurement.

A. Preprocessing

The terrain in forests shows significant variations in height and contains substantial under-canopy vegetation. Our segmentation approach considers no semantics and is aimed solely at identifying trees. We preprocess an input point cloud with the aim of filtering out the ground, bushes, and any small near-ground structures. We first minimally denoise the cloud and apply the cloth simulation algorithm proposed by Zhang et al. [45] to compute a ground segmentation. Their method inverts the z-axis of the point cloud $\mathcal{P}$ and simulates the interaction of a rigid cloth covering the inverted ground surface, extracting the set of ground points $\mathcal{P}^G$.

For points $\mathbf{p} = [p_x, p_y, p_z]^\top \in \mathcal{P}$ and $\mathbf{p}^i \in \mathcal{P}^G$, we interpolate the ground elevation of a point $h(\mathbf{p})$ as

$$h(\mathbf{p}) = \frac{\sum_{\mathbf{p}^i \in \mathcal{N}} w(\mathbf{p}, \mathbf{p}^i) p_z^i}{\sum_{\mathbf{p}^i \in \mathcal{N}} w(\mathbf{p}, \mathbf{p}^i)} \tag{1}$$

$$w(\mathbf{p}, \mathbf{p}^i) = d_{xy}(\mathbf{p}, \mathbf{p}^i)^{-2}, \tag{2}$$

where $d_{xy}(\mathbf{p}, \mathbf{p}^i)$ is the L2 norm over the x-y coordinates of the points, which is also used to define the local neighborhood $\mathcal{N}$ around a point $\mathbf{p}$. We subtract $h(\mathbf{p})$ from p_z of each point, producing an elevation or height normalized point cloud. We then clip out points below 1 m in z-height to remove undergrowth vegetation. An example result of the ground segmentation and height normalization is given in Fig. 2.

B. Tree Instance Segmentation

Following existing methods [1], [17], [30], we downsample the height-normalized cloud to remove duplicate points and speed up the segmentation. The size of voxelization is a parameter that can influence the upper bound of accuracy as desired. However, we note that the accuracy of DBH estimation typically falls within the range of 1 to 4 centimeters [20].

As the core of our segmentation approach, we apply Quickshift++ [14], a modification of the original Quickshift

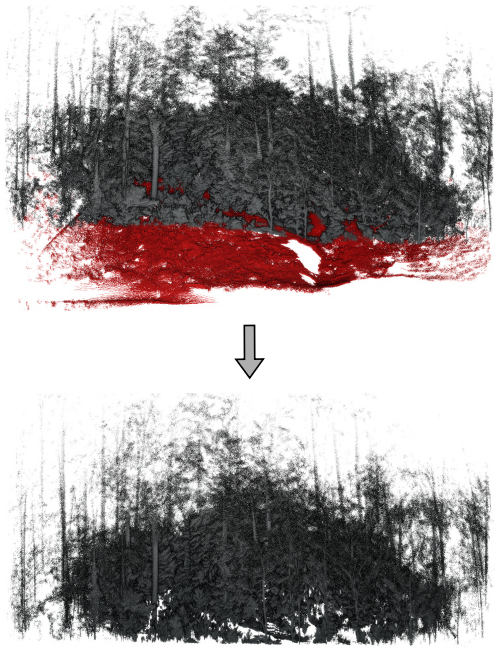

Fig. 2: Results of ground segmentation and height normalization steps. In the top image, points in red denote identified ground points. The ground segmentation is used to normalize the height, as shown in the image below.

density-based clustering algorithm [39]. Following is a brief summary of Quickshift++ while illustrating how we use it in the context of our problem. For more details, we refer the reader to the work by Jiang et al. [14].

Let $r_k(\mathbf{p})$ for a point $\mathbf{p} \in \mathcal{P}$ be the distance of $\mathbf{p}$ to its k-th nearest neighbor. For the true density $f(\mathbf{p})$ of a point $\mathbf{p}$, the k-NN density estimate of it is defined as

$$f_k(\mathbf{p}) = \frac{k}{n\, v\, r_k(\mathbf{p})^3}, \tag{3}$$

where n is the number of points in $\mathcal{P}$ and v is the volume of a unit ball in $\mathbb{R}^3$. In the first step, Quickshift++ aims at identifying the modes of $f(\mathbf{p})$ as cluster cores. These modes represent regions of locally high density. We define the mutual k-NN graph $G(\lambda)$ for a density level λ with vertices $\mathcal{V}$ and edges $\mathcal{E}$ as

$$\mathcal{V} = \{\mathbf{p} \in \mathcal{P} \mid f_k(\mathbf{p}) \geq \lambda\} \tag{4}$$

$$\mathcal{E} = \{\{\mathbf{p}_i, \mathbf{p}_j\} \mid \|\mathbf{p}_i - \mathbf{p}_j\| \leq \min(r_k(\mathbf{p}_i), r_k(\mathbf{p}_j))\}. \tag{5}$$

The connected components of $G(\lambda)$ approximate the connected components of the λ-level sets of the true density $f(\mathbf{p})$. If the λ-levels of $G(\lambda)$ are scanned top-down, every new distinct connected component that appears corresponds to a local maxima at approximately density level λ. By then taking the corresponding connected components instead in $G((1-\beta)\lambda)$, with the $(1-\beta)$ multiplicative factor allowing for fluctuations in local density, we can identify cluster cores as the regions surrounding local modes.

In our pipeline, we take a top-down approach to tree segmentation. We first project the height-normalized cloud onto the XY-plane, similarly to Nelson et al. [28]. We

Fig. 3: An image of one of the forest plots in Switzerland. April tags are placed on individual trees to allow easy association of the measured traits.

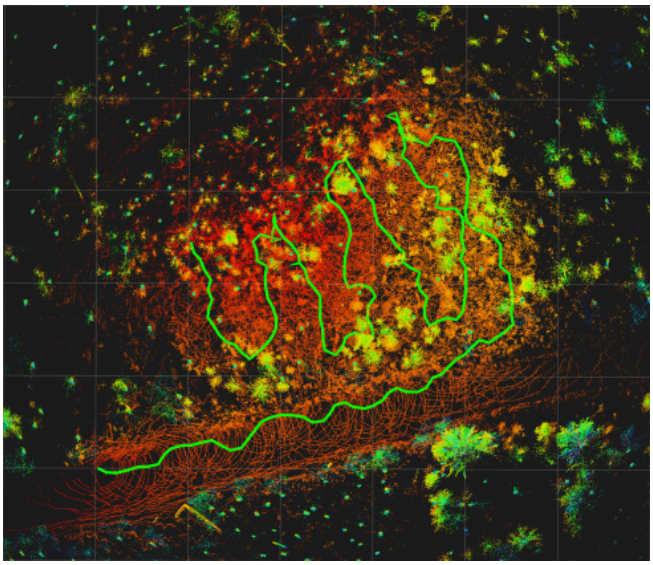

Fig. 4: The trajectory followed by the ANYmal robot during data collection in the forest near Evo, Finland. The platform was equipped with a Velodyne VLP-16.

then identify the core sets, reasoning that the trunks should primarily correspond to the densest regions. These cluster core sets are unprojected back to their corresponding 3D points. Subsequently, the remaining points are clustered via the second step of Quickshift++ wherein each point is moved closer to its nearest neighbor with the highest density $f_k(\mathbf{p})$ until it reaches some cluster core. The two main parameters of the approach are k for the k-th nearest neighbor and β for the fluctuation in density allowed in a cluster.

C. Geometric Primitive Fitting

For each point to be assigned to an instance, we filter out the points with a height between 1 m and 4 m. We then fit a cylinder following a RANSAC scheme, where we first sample five points and calculate the corresponding mean $\boldsymbol{\mu}$ and covariance matrix $\boldsymbol{\Sigma}$. The mean defines the center of the cylinder, the eigenvector corresponding to the largest eigenvalue of $\boldsymbol{\Sigma}$ defines its axis $\mathbf{a}$, and the square root of the second-largest eigenvalue defines the radius r. We define the error e_p per point as

$$e_p = \|\mathbf{a} \times (\mathbf{p} - \boldsymbol{\mu})\|_2 - r. \tag{6}$$

We take as inliers the points for which the error is less than 10% of the voxel size. Using this estimate as an initial guess, we then refine it through a least-squares minimization scheme. The DBH of a tree is then simply the diameter of the estimated cylinder. While some approaches [13], [30] first filter out points close to the nominal DBH height (1.3 m) and then fit a circle to the points, we find from our experiments (Sec. IV-C) a strong agreement with reference measurements with this alternative approach as well.

IV. Experimental Evaluation

The main focus of this work is a pipeline to support automated forest inventory using mobile robotic laser scanning platforms. We present here our experiments showing the capabilities of our method to segment trees and compute the DBH for every tree. The results of our experiments as presented below also support our key claims, which are: (i) strong performance in tree instance segmentation on mobile laser scans of forests, (ii) strong estimation of tree DBH through cylinder fitting, achieving high accuracy for forest inventory, and (iii) solid qualitative performance across data from varied sensor types with simple tuning.

A. Experimental Setup

We carried out field campaigns and collected extensive data from forests near Stein am Rhein, Switzerland, and Evo, Finland during March and May 2023 respectively under the supervision of the Swiss Federal Institute for Forest, Snow, and Landscape Research. LiDAR sensor rigs included a Hesai Pandar XT-32, Leica's BLK sensors, and the ANYmal robotic platform mounted with a Velodyne VLP-16. We show qualitative results on data from across these sensors and forests and focus our quantitative evaluation on the data collected from the Hesai sensor during the Switzerland campaign. Before mapping or measuring the trees, we attached April tags to the barks of the trees under study, noting the tag ID alongside any tree traits measured. This allowed a simplified association of the traits to laser scans by detecting the tags from RGB cameras attached to the Hesai sensor, giving a pose estimate of each tree in the map frame. With our approach, we aimed to keep the need for manual labeling of point cloud data, which is a tedious task, to as minimal as possible. However, we did label point clouds from 5 forest plots consisting of 143 individual tree instances, focusing on labeling only the trees for which ground truth traits were measured. Of this, we take a single forest plot with 13 labeled trees to optimize the parameters of our approach (two parameters) and those of the baselines when feasible. This plot is not included in testing, and we report the results in the following sections from experiments on the other four forest plots. We note that such an optimization step is completely optional in normal usage, and necessary only for fine-tuning.

Method	Plot 1	Plot 2	Plot 3	Plot 4	Average
Silva et al. [36]	0.197	0.355	0.163	0.384	0.275
Dalponte et al. [5]	0.194	0.365	0.159	0.400	0.280
Li et al. [18]	0.390	0.485	0.341	0.535	0.437
Donager et al. [7]	0.612	0.561	0.330	0.485	0.497
Ours	**0.761**	**0.722**	**0.489**	**0.781**	**0.688**

TABLE I: Evaluation of instance segmentation of different approaches comparing panoptic quality (PQ).

Method	Plot 1	Plot 2	Plot 3	Plot 4	Average
Donager et al. [7]	2.988	2.721	2.963	-	2.890
Krisanksi et al. [16]	**0.031**	**0.051**	**0.100**	**0.021**	**0.051**
Ours	0.088	0.116	0.182	0.054	0.110

TABLE II: Comparison of DBH estimation performance in RMSE (m) of different algorithms.

B. Instance Segmentation

The first experiment evaluates the performance of our instance segmentation approach. Its outcome supports the claim that we can accurately delineate trees along with their canopies into individual instances. We show comparisons against the methods of Silva et al. [36], Dalponte et al. [5], Li et al. [18], and Donager et al. [7]. The motivation for these baselines is that, in part, they are state-of-the-art methods, but also that their working implementation is available open-source. We do not compare against the results of Krisanski et al. [16] since their method does not perform canopy separation. For the forest plots under study, DBH measurements were collected only for a subset of trees in each plot. We labeled only this subset of trees, resulting in a dataset containing partially annotated point clouds. To then evaluate the segmentation performance of the approaches, we use the standard panoptic quality (PQ) metric [4], [15]. PQ is given by

$$\mathrm{PQ} = \frac{\sum_{(p,g)\in \mathrm{TP}} \mathrm{IoU}(p,g)}{|\mathrm{TP}| + \frac{1}{2}|\mathrm{FP}| + \frac{1}{2}|\mathrm{FN}|} \tag{7}$$

where p, g represent the predicted and ground truth instance labels, TP is the set of true positives, FP is the set of false positives, FN is the set of false negatives, IoU is the intersection over union, and $|S|$ represents the cardinality of the set S. This metric measures how well are the points assigned to their instances allowing us to evaluate the methods with respect to the partial ground truth annotations.

Tab. I shows a quantitative comparison of our approach against the baselines. We see that our approach outperforms the baselines by a substantial margin. We show further qualitative results of our approach in Sec. IV-D.

C. Tree Trait Estimation

The second experiment evaluates the tree trait estimation and illustrates that our approach can estimate DBH to produce an accurate forest inventory. We take the methods of Donager et al. [7] and Krisanski et al. [16] as baselines for DBH estimation and report the root-mean-square error (RMSE) values.

Tab. II presents a quantitative comparison of our approach against the baselines. As we can see from the results, our approach achieves around 11.8 cm RMSE in the DBH estimation. While we do not perform on-par with the approach of Krisanski et al. [16], their method exploits semantic segmentation to include only the tree's stem into each instance, excluding any canopy or undergrowth vegetation. Our method, however, segments also the tree's canopy along with the stem into each instance. Moreover, since we do not have semantic information, we potentially segment the bushes and undergrowth vegetation along with the canopy. To mitigate this, we clip the height-normalized point cloud below 1 m as a pre-processing step to remove such vegetation but we still found it insufficient in the forest plots that we studied. Simply clipping more of the cloud also renders the DBH estimation inefficient, as this is typically measured at around 1.3 m. As a consequence, our cylinder fitting strategy is not restricted to the stem, which degrades the performance in terms of the DBH estimation. Notice, however, that the gap in estimation accuracy is, on average, below 6 cm. The other geometric method proposed by Donager et al. [7] fails on this data with an average RMSE of 2.89 m. We exclude the result for Plot 4 from the average and in Tab. II since, in this case, Donager et al. [7] estimate an average DBH of over 300 meters. This is due to many outliers in their tree instance segmentation. We notice that, in general, the rather low performance of Donager et al. [7] stems from their instance segmentation method overestimating the number of trees in each forest plot, highlighting the importance of instance segmentation in forestry traits estimation.

D. Qualitative Performance of Our Approach

We show in Fig. 5 the result of our approach to cylinder fitting on a forest plot in Evo, Finland. Furthermore, in Fig. 6, we present the qualitative analysis of our pipeline showcasing the robustness of our approach. Note that the data for these experiments was collected from several sensors and from different geographical locations, i.e., forests in Switzerland and Finland.

In summary, our evaluation suggests that our method is applicable for producing forest inventory from data collected with mobile robotic platforms, providing accurate segmentation of trees and DBH estimation. The method is robust and requires minimal effort to be adapted to a different sensor or geographical region. Thus, we supported all our claims with this experimental evaluation.

V. Conclusion

In this paper, we presented a novel approach to instance segmentation of forest scenes mapped using mobile laser scanning platforms and subsequent estimation of per-tree traits. Our approach has only a handful of parameters, making it simple to tune and adapt. We implemented and quantitatively evaluated our approach on data collected using a mobile robotics sensor rig from a forest in Switzerland. Furthermore, we showcase good qualitative performance on

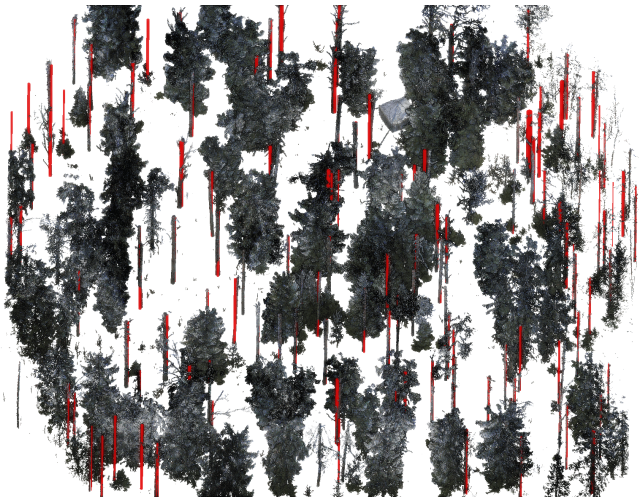

Fig. 5: Qualitative results of our cylinder fitting approach. Cylinders are shown in red. The point cloud has been cropped along its height to allow clearer visualization.

data collected in an entirely different type of forest in Finland and also on data from varied sensor setups. We provided comparisons to other existing techniques and supported all claims made in this paper. The experiments suggest that our approach has the potential to vastly speed up the generation of accurate inventory of wide expanses of forests, taking advantage of the cost-effectiveness and flexibility of mobile robotic platforms. Our approach outperforms popular existing baseline methods for tree instance segmentation. In future work, we aim to introduce semantics in our pipeline to distinguish between canopy, stem and undergrowth vegetation and further improve the DBH estimation.

Acknowledgments

We thank Saurabh Gupta for proofreading the manuscript and providing visualizations of the results. We thank Leica Geosystems AG for supporting us with the BLK sensors. We thank also PreFor Oy and especially Henri Riihimäki for their assistance during the Finland data collection campaign. We thank Christian Ginzler and his remote sensing team from WSL for supporting the data collection in Switzerland by providing the drone DJI M600 and the TLS Rigl VZ-400i.

References

[1] A. Burt, M. Disney, and K. Calders. Extracting individual trees from lidar point clouds using treeseg. *Methods in Ecology and Evolution*, 10(3):438–445, 2019.

[2] N. Chebrolu, T. Läbe, O. Vysotska, J. Behley, and C. Stachniss. Adaptive Robust Kernels for Non-Linear Least Squares Problems. *IEEE Robotics and Automation Letters (RA-L)*, 6:2240–2247, 2021.

[3] S.W. Chen, G.V. Nardari, E.S. Lee, C. Qu, X. Liu, R.A.F. Romero, and V. Kumar. Sloam: Semantic lidar odometry and mapping for forest inventory. *IEEE Robotics and Automation Letters (RA-L)*, 5(2):612–619, 2020.

[4] B. Cheng, I. Misra, A.G. Schwing, A. Kirillov, and R. Girdhar. Masked-attention mask transformer for universal image segmentation. In *Proc. of the IEEE/CVF Conf. on Computer Vision and Pattern Recognition (CVPR)*, 2022.

[5] M. Dalponte and D.A. Coomes. Tree-centric mapping of forest carbon density from airborne laser scanning and hyperspectral data. *Methods in Ecology and Evolution*, 7(10):1236–1245, 2016.

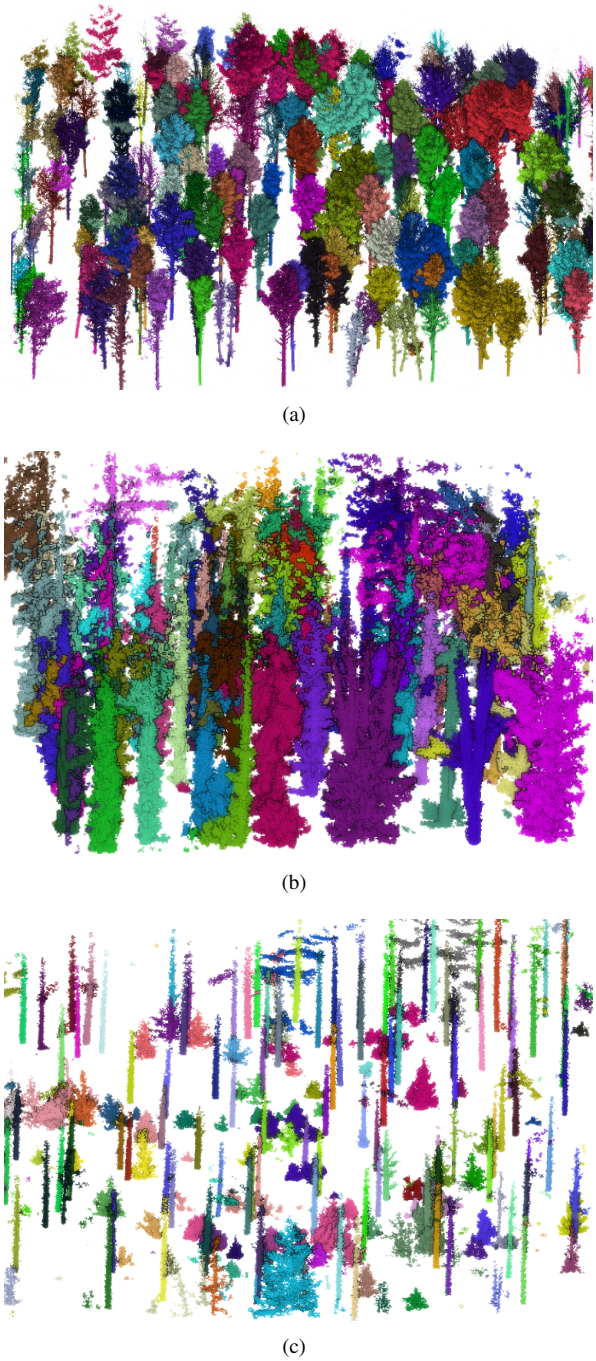

(a)

(b)

(c)

Fig. 6: Qualitative results of our tree instance segmentation pipeline. (a) shows the instance segmentation for the Leica's BLK sensor on the Evo site in Finland, (b) for the Hesai LiDAR in the Switzerland site, and (c) for the ANYmal platform in the Evo site.

[6] J.G. de Tanago, A. Lau, H. Bartholomeus, M. Herold, V. Avitabile, P. Raumonen, C. Martius, R.C. Goodman, M. Disney, S. Manuri, A. Burt, and K. Calders. Estimation of above-ground biomass of large tropical trees with terrestrial lidar. *Methods in Ecology and Evolution*, 9(2):223–234, 2018.

[7] J.J. Donager, A.J.S. Meador, and R.C. Blackburn. Adjudicating perspectives on forest structure: How do airborne, terrestrial, and mobile lidar-derived estimates compare? *Remote Sensing*, 13(12), 2021.

[8] S. Du, R. Lindenbergh, H. Ledoux, J. Stoter, and L. Nan. Adtree: Accurate, detailed, and automatic modelling of laser-scanned trees.

Remote Sensing, 11(18), 2019.

[9] J.M. Fortin, O. Gamache, V. Grondin, F. Pomerleau, and P. Giguère. Instance segmentation for autonomous log grasping in forestry operations. In *Proc. of the IEEE/RSJ Intl. Conf. on Intelligent Robots and Systems (IROS)*, 2022.

[10] P.D. Frenne, J. Lenoir, M. Luoto, B.R. Scheffers, F. Zellweger, J. Aalto, M.B. Ashcroft, D.M. Christiansen, G. Decocq, K.D. Pauw, S. Govaert, C. Greiser, E. Gril, A. Hampe, T. Jucker, D.H. Klinges, I.A. Koelemeijer, J.J. Lembrechts, R. Marrec, C. Meeussen, J. Ogée, V. Tyystjärvi, P. Vangansbeke, and K. Hylander. Forest microclimates and climate change: Importance, drivers and future research agenda. *Global Change Biology*, 27(11):2279–2297, 2021.

[11] G. Grisetti, R. Kümmerle, C. Stachniss, and W. Burgard. A tutorial on graph-based SLAM. *IEEE Trans. on Intelligent Transportation Systems Magazine*, 2:31–43, 2010.

[12] S. Gupta, T. Guadagnino, B. Mersch, I. Vizzo, and C. Stachniss. Effectively Detecting Loop Closures using Point Cloud Density Maps. In *Proc. of the IEEE Intl. Conf. on Robotics & Automation (ICRA)*, 2024.

[13] H.K. Heo, D.K. Lee, J.H. Park, and J.H. Thorne. Estimating the heights and diameters at breast height of trees in an urban park and along a street using mobile lidar. *Landscape and Ecological Engineering*, 15(3):253–263, 2019.

[14] H. Jiang, J. Jang, and S. Kpotufe. Quickshift++: Provably good initializations for sample-based mean shift. In *Proc. of the Intl. Conf. on Machine Learning (ICML)*, 2018.

[15] A. Kirillov, K. He, R. Girshick, C. Rother, and P. Dollár. Panoptic Segmentation. In *Proc. of the IEEE/CVF Conf. on Computer Vision and Pattern Recognition (CVPR)*, 2019.

[16] S. Krisanski, M.S. Taskhiri, S.G. Aracil, D. Herries, A. Muneri, M.B. Gurung, J. Montgomery, and P. Turner. Forest structural complexity tool—an open source, fully-automated tool for measuring forest point clouds. *Remote Sensing*, 13(22), 2021.

[17] S. Krisanski, M.S. Taskhiri, S.G. Aracil, D. Herries, and P. Turner. Sensor agnostic semantic segmentation of structurally diverse and complex forest point clouds using deep learning. *Remote Sensing*, 13(8), 2021.

[18] W. Li, Q. Guo, M.K. Jakubowski, and M. Kelly. A new method for segmenting individual trees from the lidar point cloud. *Photogrammetric Engineering and Remote Sensing (PE&RS)*, 78(1):75–84, 2012.

[19] X. Liang, J. Hyyppä, H. Kaartinen, M. Lehtomäki, J. Pyörälä, N. Pfeifer, M. Holopainen, G. Brolly, P. Francesco, J. Hackenberg, H. Huang, H.W. Jo, M. Katoh, L. Liu, M. Mokroš, J. Morel, K. Olofsson, J. Poveda-Lopez, J. Trochta, D. Wang, J. Wang, Z. Xi, B. Yang, G. Zheng, V. Kankare, V. Luoma, X. Yu, L. Chen, M. Vastaranta, N. Saarinen, and Y. Wang. International benchmarking of terrestrial laser scanning approaches for forest inventories. *ISPRS Journal of Photogrammetry and Remote Sensing (JPRS)*, 144:137–179, 2018.

[20] X. Liang, V. Kankare, J. Hyyppä, Y. Wang, A. Kukko, H. Haggrén, X. Yu, H. Kaartinen, A. Jaakkola, F. Guan, M. Holopainen, and M. Vastaranta. Terrestrial laser scanning in forest inventories. *ISPRS Journal of Photogrammetry and Remote Sensing (JPRS)*, 115:63–77, 2016.

[21] M. Liu, Z. Feng, Z. Zhang, C. Ma, M. Wang, B. ling Lian, R. Sun, and L. Zhang. Development and evaluation of height diameter at breast models for native chinese metasequoia. *PLOS ONE*, 12(8):1–16, 2017.

[22] X. Liu, G.V. Nardari, F.C. Ojeda, Y. Tao, A. Zhou, T. Donnelly, C. Qu, S.W. Chen, R.A.F. Romero, C.J. Taylor, and V. Kumar. Large-scale autonomous flight with real-time semantic slam under dense forest canopy. *IEEE Robotics and Automation Letters*, 7(2):5512–5519, 2022.

[23] J.A. Lutz, T.J. Furniss, D.J. Johnson, S.J. Davies, D. Allen, A. Alonso, K.J. Anderson-Teixeira, A. Andrade, J. Baltzer, K.M.L. Becker, E.M. Blomdahl, N.A. Bourg, S. Bunyavejchewin, D.F.R.P. Burslem, C.A. Cansler, K. Cao, M. Cao, D. Cárdenas, L.W. Chang, K.J. Chao, W.C. Chao, J.M. Chiang, C. Chu, G.B. Chuyong, K. Clay, R. Condit, S. Cordell, H.S. Dattaraja, A. Duque, C.E.N. Ewango, G.A. Fischer, C. Fletcher, J.A. Freund, C. Giardina, S.J. Germain, G.S. Gilbert, Z. Hao, T. Hart, B.C.H. Hau, F. He, A. Hector, R.W. Howe, C.F. Hsieh, Y.H. Hu, S.P. Hubbell, F.M. Inman-Narahari, A. Itoh, D. Janík, A.R. Kassim, D. Kenfack, L. Korte, K. Král, A.J. Larson, Y. Li, Y. Lin, S. Liu, S. Lum, K. Ma, J.R. Makana, Y. Malhi, S.M. McMahon, W.J. McShea, H.R. Memiaghe, X. Mi, M. Morecroft, P.M. Musili, J.A. Myers, V. Novotny, A. de Oliveira, P. Ong, D.A. Orwig, R. Ostertag, G.G. Parker, R. Patankar, R.P. Phillips, G. Reynolds, L. Sack, G.Z.M. Song, S.H. Su, R. Sukumar, I.F. Sun, H.S. Suresh, M.E. Swanson, S. Tan, D.W. Thomas, J. Thompson, M. Uriarte, R. Valencia, A. Vicentini, T. Vrška, X. Wang, G.D. Weiblen, A. Wolf, S.H. Wu, H. Xu, T. Yamakura, S. Yap, and J.K. Zimmerman. Global importance of large-diameter trees. *Global Ecology and Biogeography*, 27(7):849–864, 2018.

[24] C. Malzer and M. Baum. A hybrid approach to hierarchical density-based cluster selection. In *Intl. Conf. on Multisensor Fusion and Integration for Intelligent Systems (MFI)*, 2020.

[25] E. Marks, M. Sodano, F. Magistri, L. Wiesmann, D. Desai, R. Marcuzzi, J. Behley, and C. Stachniss. High precision leaf instance segmentation for phenotyping in point clouds obtained under real field conditions. *IEEE Robotics and Automation Letters (RA-L)*, 8(8):4791–4798, 2023.

[26] S.M.K. Moorthy, K. Calders, M.B. Vicari, and H. Verbeeck. Improved supervised learning-based approach for leaf and wood classification from lidar point clouds of forests. *IEEE Trans. on Geoscience and Remote Sensing*, 58(5):3057–3070, 2020.

[27] A.S. Mori, K.P. Lertzman, and L. Gustafsson. Biodiversity and ecosystem services in forest ecosystems: a research agenda for applied forest ecology. *Journal of Applied Ecology*, 54(1):12–27, 2017.

[28] H.J. Nelson and N. Papanikolopoulos. Pre-clustering point clouds of crop fields using scalable methods. *arXiv preprint*, arXiv:2107.10950, 2022.

[29] L. Pellissier, M. Anzini, L. Maiorano, A. Dubuis, J. Pottier, P. Vittoz, and A. Guisan. Spatial predictions of land-use transitions and associated threats to biodiversity: the case of forest regrowth in mountain grasslands. *Applied Vegetation Science*, 16(2):227–236, 2013.

[30] A. Proudman, M. Ramezani, S. Digumarti, N. Chebrolu, and M. Fallon. Towards real-time forest inventory using handheld LiDAR. *Journal on Robotics and Autonomous Systems (RAS)*, 157, 2022.

[31] C. Qi, K. Yi, H. Su, and L.J. Guibas. PointNet++: Deep Hierarchical Feature Learning on Point Sets in a Metric Space. In *Proc. of the Conf. on Neural Information Processing Systems (NeurIPS)*, 2017.

[32] M. Ramezani, M. Mattamala, and M. Fallon. AEROS: AdaptivE RObust Least-Squares for Graph-Based SLAM. *Frontiers in Robotics and AI*, 2022.

[33] G. Roggiolani, M. Sodano, T. Guadagnino, F. Magistri, J. Behley, and C. Stachniss. Hierarchical approach for joint semantic, plant instance, and leaf instance segmentation in the agricultural domain. In *Proc. of the IEEE Intl. Conf. on Robotics & Automation (ICRA)*, 2023.

[34] J.R. Roussel, D. Auty, N.C. Coops, P. Tompalski, T.R. Goodbody, A.S. Meador, J.F. Bourdon, F. de Boissieu, and A. Achim. lidr: An r package for analysis of airborne laser scanning (als) data. *Remote Sensing of Environment*, 251:112061, 2020.

[35] F. Schiefer, T. Kattenborn, A. Frick, J. Frey, P. Schall, B. Koch, and S. Schmidtlein. Mapping forest tree species in high resolution uav-based rgb-imagery by means of convolutional neural networks. *ISPRS Journal of Photogrammetry and Remote Sensing (JPRS)*, 170:205–215, 2020.

[36] C.A. Silva, A.T. Hudak, L.A. Vierling, E.L. Loudermilk, J.J. O'Brien, J.K. Hiers, S.B. Jack, C. Gonzalez-Benecke, H. Lee, M.J. Falkowski, and A. Khosravipour. Imputation of individual longleaf pine (pinus palustris mill.) tree attributes from field and lidar data. *Canadian Journal of Remote Sensing*, 42(5):554–573, 2016.

[37] C. Stachniss, J. Leonard, and S. Thrun. *Springer Handbook of Robotics, 2nd edition*, chapter Chapt. 46: Simultaneous Localization and Mapping. Springer Verlag, 2016.

[38] C. Sun, C. Huang, H. Zhang, B. Chen, F. An, L. Wang, and T. Yun. Individual tree crown segmentation and crown width extraction from a heightmap derived from aerial laser scanning data using a deep learning framework. *Frontiers in Plant Science*, 13, 2022.

[39] A. Vedaldi and S. Soatto. Quick shift and kernel methods for mode seeking. In *Proc. of the Europ. Conf. on Computer Vision (ECCV)*, 2008.

[40] I. Vizzo, T. Guadagnino, B. Mersch, L. Wiesmann, J. Behley, and C. Stachniss. KISS-ICP: In Defense of Point-to-Point ICP – Simple, Accurate, and Robust Registration If Done the Right Way. *IEEE Robotics and Automation Letters (RA-L)*, 8(2):1029–1036, 2023.

[41] O. Vysotska and C. Stachniss. Lazy Data Association For Image Sequences Matching Under Substantial Appearance Changes. *IEEE Robotics and Automation Letters (RA-L)*, 1(1):213–220, 2016.

[42] D. Wang, S.M. Takoudjou, and E. Casella. Lewos: A universal leaf-wood classification method to facilitate the 3d modelling of large

tropical trees using terrestrial lidar. *Methods in Ecology and Evolution*, 11(3):376–389, 2020.

[43] H. Weiser, J. Schäfer, L. Winiwarter, N. Kra šovec, F.E. Fassnacht, and B. Höfle. Individual tree point clouds and tree measurements from multi-platform laser scanning in german forests. *Earth System Science Data*, 14(7):2989–3012, 2022.

[44] M.A. Wulder, J.C. White, R.F. Nelson, E. Næsset, H.O. Ørka, N.C. Coops, T. Hilker, C.W. Bater, and T. Gobakken. Lidar sampling for large-area forest characterization: A review. *Remote Sensing of Environment*, 121:196–209, 2012.

[45] W. Zhang, J. Qi, P. Wan, H. Wang, D. Xie, X. Wang, and G. Yan. An easy-to-use airborne lidar data filtering method based on cloth simulation. *Remote Sensing*, 8(6), 2016.

CERTIFICATE OF REPRODUCIBILITY

The authors of this publication declare that:

1) The software related to this publication is distributed in the hope that it will be useful, support open research, and simplify the reproducability of the results but it comes without any warranty and without even the implied warranty of merchantability or fitness for a particular purpose.

2) *Meher Malladi* primarily developed the implementation related to this paper. This was done on Ubuntu 22.04.

3) *Luca Lobefaro* verified that the code can be executed on a machine that follows the software specification given in the Git repository available at:

   `https://github.com/PRBonn/forest_inventory_pipeline`

4) *Luca Lobefaro* verified that the experimental results presented in this publication can be reproduced using the implementation used at submission, which is labeled with a tag in the Git repository and can be retrieved using the command:

   `git checkout ICRA2024`